

Cite this: *RSC Chem. Biol.*, 2025,
6, 1779

A trifunctional probe for generation of fluorogenic glycan-photocrosslinker conjugates

Brandon Vreulz, Daphnée De Crozals and Samy Cecioni *

Interactions between cell surface glycans and lectins mediate vital biological processes, yet their characterization is hindered by the low affinity of these binding events. While photoaffinity labeling can capture these interactions, traditional custom probes often demand tedious synthesis, are limited to simple glycans, and lack versatility. To overcome these limitations, we report a trifunctional scaffold enabling modular assembly of glycan probes. This scaffold integrates orthogonal sites for: (i) efficient late-stage ligation of native oligosaccharides via an *N*-alkoxy-amine, preserving glycan structure; (ii) flexible amide coupling of various photocrosslinkers, including a recently developed fluorogenic azidocoumarin for traceable labeling; and (iii) conjugation to reporter tags (e.g., biotin) or multivalent carriers through a carboxylic acid motif. We demonstrate the scaffold's utility by synthesizing probes bearing various fucosylated glycans. Probes incorporating the fluorogenic photocrosslinker achieved specific, light-induced labeling of the model lectin BamBL. The platform's adaptability was further confirmed by generating monovalent biotinylated probes displaying the photoactive glycan. This modular strategy offers a practical solution to rapidly construct advanced chemical probes, facilitating the investigation of complex glycan recognition events in diverse biological systems.

Received 7th August 2025,
Accepted 16th September 2025

DOI: 10.1039/d5cb00206k

rsc.li/rsc-chembio

Introduction

Cell surfaces and extracellular matrices are decorated with a complex layer of glycosylated molecules. Across all kingdoms of life, living cells position glycans on the front line with regards to their immediate environment. Consequently, glycan recognition by glycan-binding proteins (lectins) is essential for the healthy functioning of the cell¹ by controlling complex biological functions related to cell–cell adhesion,^{2,3} cell signaling or immune responses.⁴ Concurrently, alterations of glycosylation and glycan recognition are now demonstrated hallmarks of numerous monogenic and chronic human diseases,^{5–7} but can also drive cancer malignancy⁸ as well as the adhesion of various pathogens to human tissues.⁹

Despite the relevance of glycan recognition to human health, understanding how glycans interact with glycan-binding proteins remains technically challenging. Indeed, capturing and visualizing these relatively weak, non-covalent interactions is often a major bottleneck in glycoscience research.¹⁰ Recent conceptual improvement have included metabolically incorporated sugar analogs,^{11–14} exo-enzymatic glycan labeling,^{15,16} and liquid glycan or lectin arrays through phage display.^{17–19} However, chemical photoaffinity probes^{20–22} are still often needed to create covalent

bonds between interacting partners, thereby freezing and capturing glycan recognition events. Typical designs of such photoaffinity labeling probes include a sugar recognition motif, a photocrosslinker and a chemical tag for detection and/or pull-down (e.g., biotin).^{20,23} Notable examples include bifunctional diazirine-biotin probes to capture proteins binding to human milk oligosaccharides,²¹ benzophenone-alkyne probes conjugates to glycosaminoglycan polysaccharides,²⁴ as well as gold nanoparticles decorated with galactosides and aryl azides or benzophenones.^{25,26}

While the efficacy of such photoaffinity probes is well-established, they generally remain application-specific, requiring custom design and difficult glycosylation reactions. Consequently, chemical photoaffinity probes are often restricted to simple mono- or di-saccharides and traditional photocrosslinker motifs. While the primary specificity for a terminal monosaccharide is important, biologically-relevant specificity generally emerges from binding to larger oligosaccharides, either through direct interactions within extended binding pockets or through conformational effects.^{1,27} As a result, the physiological selectivity of most lectins is poorly understood, and identifying uncharacterized glycan-binding domains remains a significant focus in the field.²⁸

With a clear need for tools that enable systematic capture of glycan–protein recognition, linear syntheses of chemical probes that start with glycosylation of simple sugars inherently limit the landscape of readily accessible glycan probes. In addition,

Department of Chemistry, Université de Montréal, P.O. Box 6128,
Station Downtown, Montréal, Québec H3C 3J7, Canada.
E-mail: samy.cecioni@umontreal.ca



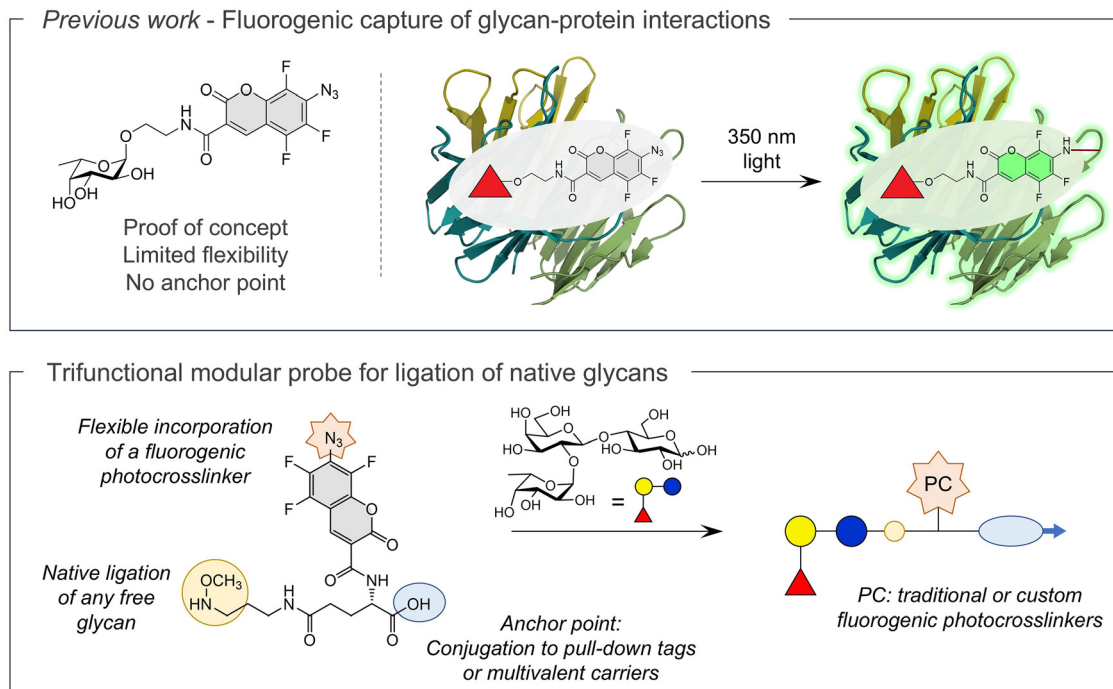


Fig. 1 Expanding fluorogenic photocrosslinking of glycan–protein interactions. Fluorogenic capture was demonstrated in 2023 by Bousch *et al.* but its design required custom chemical glycosylation reactions and did not allow for further conjugation. Here, we developed trifunctional modular probes that enable direct ligation to the reducing end of any glycan, fluorogenic photocrosslinking and conjugation to secondary tags.

the toolbox of photoreactive motifs for capturing non-covalent interacting partners has received limited conceptual improvements. While light-initiated covalent capture is attainable through traditional aryl azides, trifluoromethyldiazirines, alkyl-diazirines or benzophenones, the detection of crosslinked reaction products is not trivial. Recently, our group introduced a traceable fluorogenic photocrosslinker motif that enabled the visualization of glycan-lectin capture (Fig. 1).²⁹ To achieve fluorogenic photolabeling, we transposed the traditional aryl azide motif onto a 7-azidocoumarin scaffold and leveraged fluorination of the aromatic core to prevent nitrene rearrangements that would disrupt aromaticity.³⁰ Interestingly, highly efficient absorption with near UV light and rapid photoactivation are additional benefits of the extended conjugation on such azido-chromophores. Connecting this motif to monosaccharides, we observed a glycan-specific photolabeling that was concomitant with the permanent attachment of a fluorescent tag on crosslinked species.²⁹

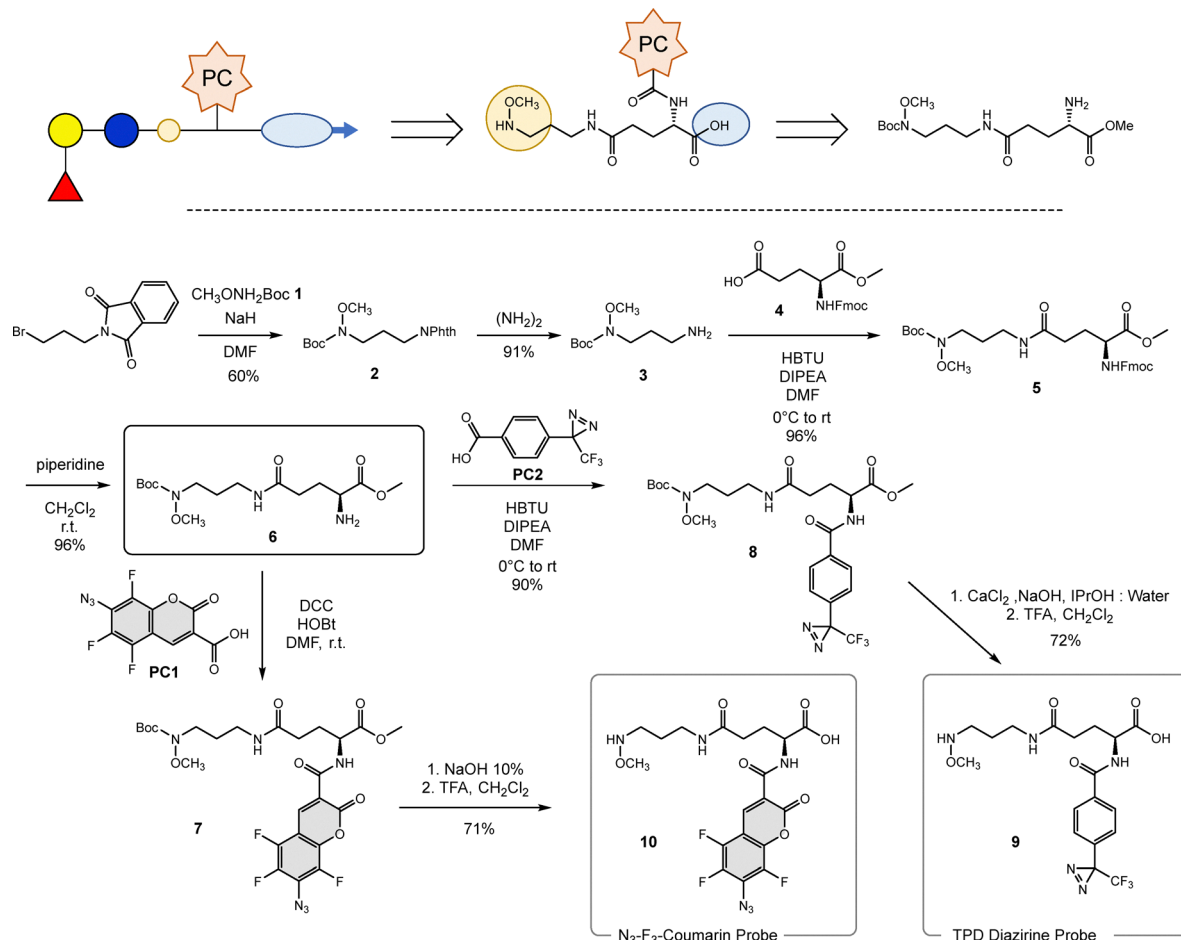
Despite having demonstrated the efficacy of this concept with lectins of various affinities, our design required specific chemical glycosylation reactions to install different sugars and did not include means to append a secondary tag for pull-down (*e.g.*, biotin). In this report, we aimed to address both the narrow applicability of common chemical probes and the lack of means for convenient traceable detection by appending our fluorogenic photocrosslinker onto a trifunctional modular scaffold. Specifically, we reasoned that a widely useful probe should enable (i) late-stage ligation of native oligosaccharides, (ii) flexible attachment of any photocrosslinker and (iii) an

anchor point either to generate monovalent tagged glycan/PC (photocrosslinker) conjugates (*e.g.*, biotin) or to present the probe onto a multivalent carrier (Fig. 1). Using methoxy-amine ligation on a trifunctional scaffold, we demonstrate efficient attachment of monosaccharides to trisaccharides, conjugation to biotin tags and fluorogenic photocrosslinking capabilities.

Results and discussion

We aimed to prepare a trifunctional scaffold bearing orthogonal groups that would enable coupling of our fluorogenic photocrosslinker as well as late-stage ligation of glycans (Scheme 1). Over the past 30 years, the field has pursued methods toward the efficient attachment of diverse glycans to chemical probes, multivalent cores and surfaces. Numerous strategies have been reported either to generate reactive glycosides or to directly anchor free oligosaccharides based on the unique reactivity of the anomeric position. When chemical transformation of glycans is practical, it is now relatively easy to prepare aminoxy-functionalized carbohydrates³¹ or to generate glycosyl azides.^{32–34} However, if one prefers to directly ligate free glycans through their reducing end, chemical probes, or surfaces, bearing hydroxylamines or hydrazides can react with the anomeric carbon in its aldehyde form. Typically, *O*-substituted hydroxylamines lead to the open-chain sugars through *E/Z* oximes, whereas hydrazides yield cyclic sugars with good stereocontrol (β -glycosides).^{35,36} Interestingly, alkylation of the hydroxylamine motif generates *N*-methoxy-iminium intermediates





Scheme 1 Synthesis of trifunctional probes. (top) Retrosynthesis of trifunctional probes. The common intermediate can be accessed in four steps from *N*-(bromopropyl)phthalimide and Fmoc-protected glutamic acid. Our modular design allows for conjugation of a novel fluorogenic coumarin photocrosslinker or a traditional trifluoromethylphenyldiazirine photocrosslinker.

Table 1 Optimization of the *N*-alkoxy-amine ligation with mono-, di- and tri-saccharides

Probe (PC)	Glycan (eq.)	Solvent/buffer	Temp (°C)	Time (h)	Yield (LCMS) (%)	NMR	
1	9 (diazirine)	Fucose (2)	DMSO/AcOH (7:3)	40	16	47	
2	9 (diazirine)	Fucose (2)	Dioxane/ammonium acetate pH 4.6	40	16	80	
3	9 (diazirine)	Fucose (2)	Dioxane/ammonium acetate pH 4.6	40	24	85	> 3:1, β:α
4	9 (diazirine)	Fucose (1.2)	Dioxane/ammonium acetate pH 4.6	40	24	72	
5	9 (diazirine)	Fucose (1.2)	Dioxane/ammonium acetate pH 4.6	60	24	75	
6	9 (diazirine)	Lactose (2)	Dioxane/ammonium acetate pH 4.6	40	48	63	β only
7	9 (diazirine)	Lactose (3)	Dioxane/ammonium acetate pH 4.6	40	48	79	β only
8	10 (N₃-couma)	Fucose (3)	Dioxane/ammonium acetate pH 5.5	40	20	81	> 3:1, β:α
9	10 (N₃-couma)	Lactose (3)	Dioxane/ammonium acetate pH 5.5	40	48	84	β only
10	10 (N₃-couma)	2'-Fucosyl-lactose (3)	Dioxane/ammonium acetate pH 5.5	40	48	79	β only
11	10 (N₃-couma)	3-Fucosyl-lactose (3)	Dioxane/ammonium acetate pH 5.5	40	48	79	β only



that readily cyclize to provide neopyranosides with high yields and good stereocontrol as well,^{37–40} yielding ligated glycans with preserved cyclic sugars. Therefore, *N,O*-disubstituted hydroxylamines such as *N*-alkoxy-amines or *N*-alkyl-aminooxy groups are now widely used motifs for ligation of free sugars and oligosaccharides. Recently, these functional groups have proven useful in bifunctional probes to ligate a diverse set of complex glycans (lactosides, *N*-glycans, etc.).^{40–43}

For the design of tri-functional probes, we prioritized the *N*-alkoxy-amine motif based on the excellent chemical stability of *N*-alkoxy-amino glycosides at physiological pH,⁴⁰ as well as its resistance to enzymatic hydrolysis by glycosidases.⁴⁴ Additionally, we reasoned that *N*-alkoxy-amines could be Boc-protected to enable convenient synthesis of complex probes and final deprotection toward late-stage glycan ligation. Therefore, we initiated our synthesis by installing *N*-Boc methoxy amine on *N*-(bromopropyl)phthalimide to yield intermediate **2**. Deprotection using hydrazine hydrate followed by HBTU-promoted coupling to the Fmoc-protected glutamic acid **4** afforded compound **5**, and removal of Fmoc-protection using piperidine

efficiently yielded trifunctional probe **6**. We then observed that this scaffold can be readily coupled to our azido-fluoro-coumarin fluorogenic photocrosslinker²⁹ **PC1**, and subjected to a deprotection sequence to provide the final N_3 -F₃-Coumarin probe (N_3 -Couma **10**) with excellent yields. Importantly, the common scaffold **6** can also be coupled with a traditional photocrosslinker, as exemplified by the synthesis of the trifluoromethylphenyldiazirine (TPD) probe **9** through a similar sequence.

With these trifunctional probes in hand, we then set out to optimize the chemical late-stage ligation of free sugars. In previous work using *N*-alkoxy-amines handles, large excesses (10 to 100 equivalent) of either the ligation probe, or the glycan, are often reported.^{41–43} Furthermore, the need for specialized chemical synthesis hardware and complex purifications limits the routine assembly of custom probes. Therefore, we set out to optimize our ligation conditions aiming at (i) simple experimental conditions, (ii) reasonable stoichiometry of reagents, and (iii) high yields and clean crude reaction mixtures to streamline purification.

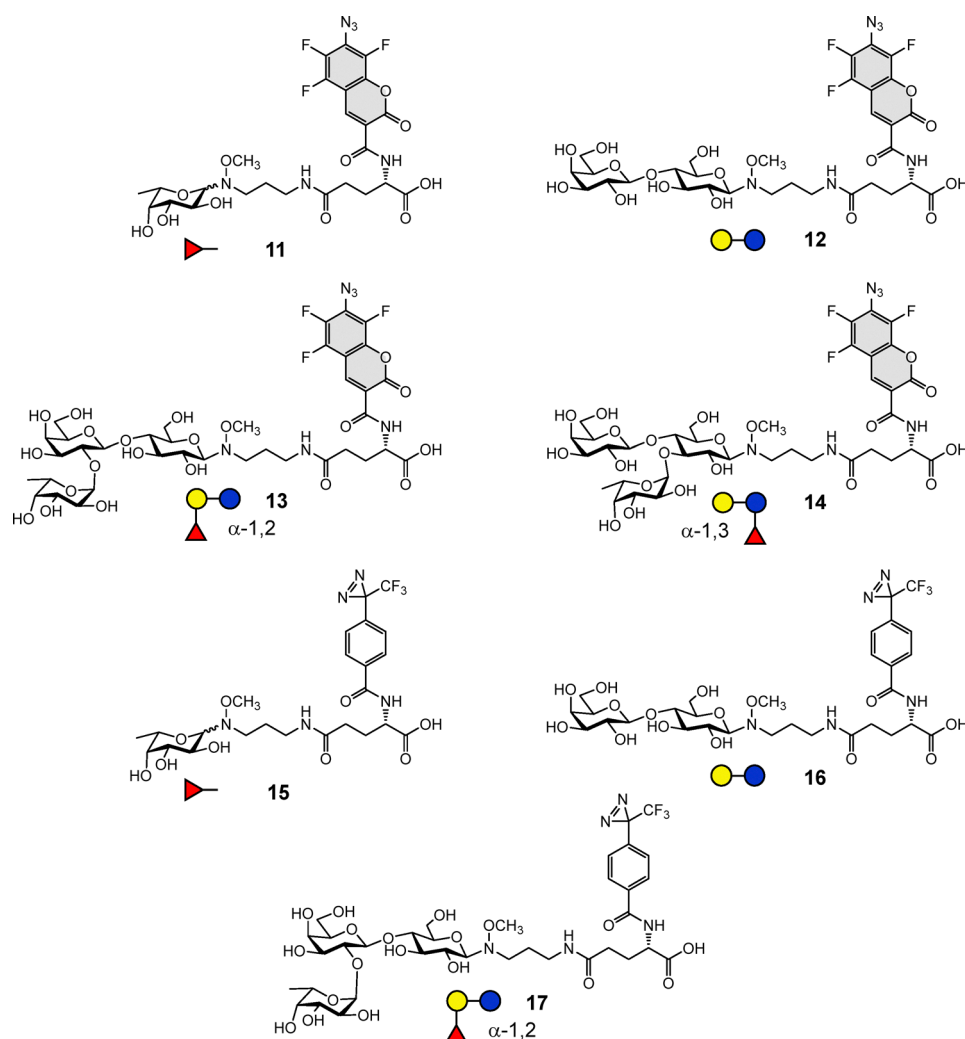


Fig. 2 Panel of fucosylated and control probes after chemical ligation.



Because we are interested in profiling fucosylated glycan recognition, we performed our optimization using a small panel of lactose and fucose-based mono-, di- and oligosaccharides. Fucose residues are installed as terminal residues on diverse glycans in mammals and are therefore important ligands for glycan-binding proteins. In addition, alterations in the fucosylated glycome occur in several diseases, though the underlying impact on glycan-lectin interactions remains poorly understood.^{45,46} Despite their relevance, only a limited number of mammalian fucose-binding lectins have been identified.⁴⁶ These include DC-SIGN, selectins and langerin lectins, which all belong to the family of C-type lectins. Interestingly, over 80 proteins with C-type lectin-like domains (CTLD) have been identified in humans, but their glycan-binding abilities remain ill-defined.^{1,47,48}

Using our diazirine-based probe, we developed a ligation protocol that can be carried out in microtubes using simple heat blocks or a PCR thermal cycler (Table 1). Screening buffers with 2 equivalents of the fucose monosaccharide, we observed 80+% yields (based on LC-MS) using a mixture of dioxane and ammonium acetate buffer at pH 4.6 (entry 2). While longer reaction times (24 h) enable near complete conversion (entry 3), we noticed that reducing the sugar stoichiometry to 1.2 equivalents had a detrimental effect on crude yields (entry 4).

Interestingly, increasing the reaction temperature from 40 °C to 60 °C improved reaction kinetics but delivered crude mixtures that contained more impurities (with fucose entry 5, or lactose see SI, Fig. S1).

Using lactose, a 48 h reaction provided the expected product with a lower yield of 63% (entry 6) but with complete beta-stereocontrol as assessed by ¹H-NMR of crude mixtures after lyophilisation. This could be remedied by using a slightly higher excess of lactose (3 eq., 79% yield, entry 7). Applying these conditions with the trifunctional probe bearing our fluorogenic photocrosslinker (N₃-Couma **10**) delivered the corresponding glycosylated probes albeit with slightly diminished reactivity. However, using 3 eq. of glycans, 48 h reactions, and an adjusted pH of 5.5 for oligosaccharides, all reactions were high yielding, demonstrating the versatility of the *N*-alkoxy-amine motif. As shown through analysis of crude reactions by LCMS, these reactions proceeded cleanly at 40 °C. Importantly, probes can be easily purified using filtration through C18 SPE cartridges (SI, Fig. S2). Finally, we tested the stability of this ligation and observed that stocks of these probes remain stable for months at -20 °C (SI, Fig. S3).

Using this strategy, we prepared a small panel of glycosylated probes in mg scales (Fig. 2). After purification, these

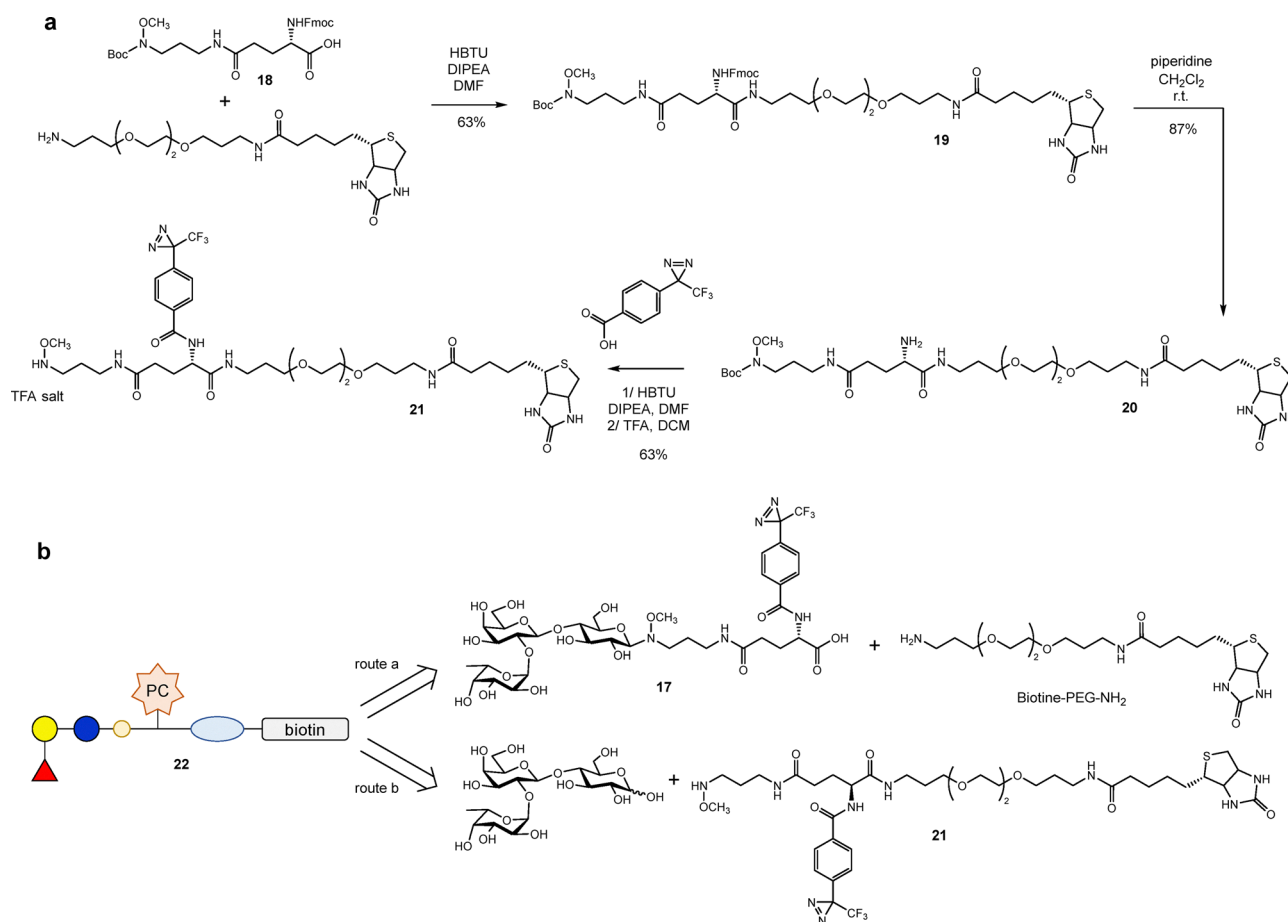


Fig. 3 (a) The modular trifunctional platform enables synthesis of biotinylated probes. (b) Through orthogonal protecting groups, one can either first biotinylate the glycosylated probes, or perform glycan ligation on a biotinylated intermediate.



probes were characterized by $^1\text{H-NMR}$, LC-MS, and HRMS (SI). This common trifunctional scaffold therefore demonstrated its ability to accommodate our custom fluorogenic photocrosslinker and to ligate various glycans efficiently. Importantly, the third anchor point consisting of a carboxylic acid remains available to generate either monovalent tagged probes or to decorate multivalent carriers. To prepare monovalent biotinylated probes, we coupled an amino-biotin linker⁴⁹ to our protected scaffold **18** (Fig. 3a). After Fmoc-deprotection using piperidine, we isolated the amine **20**, coupled a trifluoromethyl phenyl diazirine (TPD) moiety, and removed the Boc protecting group to generate a monovalent biotinylated crosslinker. Prepared in 4 steps and with a 35% overall yield from our trifunctional scaffolds, the probe **21** can be synthesized in 100 mg scale and is suitable for ligation to any glycan. Since we initially showed that glycans can be first ligated to our scaffold, we reasoned that a promising alternative route would be to use the glycosylated probe **17** bearing a free carboxylic acid and connect the amino-biotin linker. Both routes (Fig. 3b, SI) proved effective to afford the monovalent probe ligated to the 2'-fucosyl-lactose trisaccharide. Importantly, we performed photocrosslinking experiments with the biotinylated probe **22** bearing this trisaccharide. Using streptavidin-Alexa 680 fluorophore conjugates, we observed efficient traditional photocrosslinking with a model lectin (SI, Fig. S4).

Next, we set out to test the performance of our modular scaffold and the derived glycosylated probes in fluorogenic photolabeling experiments. As a model lectin, we employed BambL, which is a fucose-binding lectin found in the

opportunistic bacteria *Burkholderia ambifaria*.⁵⁰ BambL is a trimeric lectin (six-bladed β -propeller) that recognizes fucosides with a micromolar affinity, but we have recently demonstrated that our fluorogenic approach is efficient with various lectins over a wide range of K_D values.²⁹ Therefore, we tested our panel of probes bearing various fucosylated motifs (fucose, 2'-fucosyl-lactose, and 3-fucosyl-lactose) as well as a lactosylated negative control and the 1st-generation fucoside probe.²⁹ We incubated the various probes with BambL (5:1 ratio) and performed photo-irradiation experiments. Because many photo-crosslinkers are prone to non-specific labeling, it is crucial to include competitive inhibition controls (here with α -Me-fucose) to determine whether the captured interaction truly arises from specific glycan recognition. After irradiation (350 nm) for 5 minutes, SDS-PAGE and transfer onto PVDF membranes, we observed efficient fluorogenic photo-crosslinking with all fucosylated probes. Importantly, competitive inhibition showed a near complete decrease in fluorescence, and the lactose probe demonstrated the absence of non-specific crosslinking (Fig. 4). Comparing various fucosylated glycans, it appeared that probes bearing a single fucose monosaccharide yielded higher levels of fluorogenic labeling. Comparable efficacy between our 1st-generation probe and our modular scaffold supports that the photoactive residue remains appropriately positioned and that the *N*-alkoxy-amine ligation did not perturb recognition by BambL. Finally, BambL is known to bind 2'-fucosyl lactosides with affinities comparable to that of α -Me-fucose, whereas 3-fucosyl oligosaccharides usually show

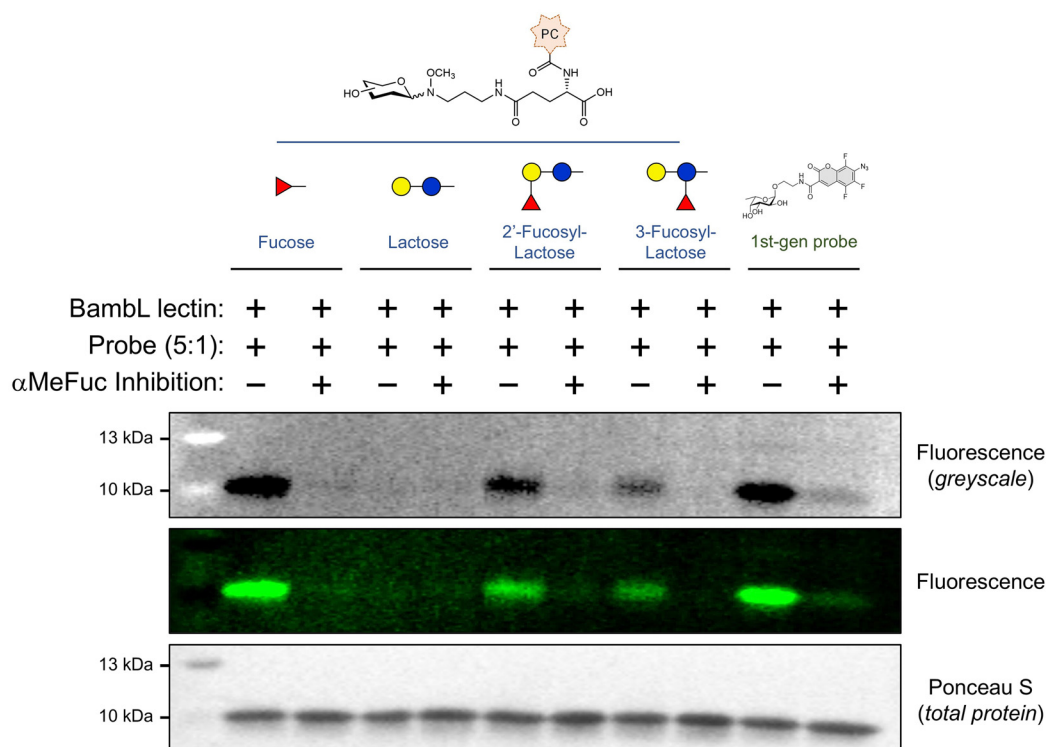


Fig. 4 Fucosylated trifunctional probes can fluorogenically crosslink a bacterial fucose-binding lectin. Performance of fucosylated probes (mono- or trisaccharides) is comparable to our 1st generation fluorogenic photocrosslinkers.



lower affinities, which is consistent with the levels of labeling observed here.⁵⁰ Correlation between fluorogenic and affinity is promising, insofar as this approach could enable the profiling of glycan preference, at the oligosaccharide level, in complex systems such as tissues or cell surfaces.

Conclusion

In this report, we present the synthesis and evaluation of a trifunctional modular scaffold that enables the ligation of complex glycans and the installation of various photocrosslinkers, including our recently reported fluorogenic photocrosslinker. This scaffold also allows further elongation toward a monovalent biotin tag and the possible display of multiple copies on multivalent carriers. In our effort toward advancing the next generation of traceable photocrosslinkers to profile glycan–protein interactions, we expect that this scaffold will be practical to readily generate libraries of glycosylated probes and novel photoactive dyes. We anticipate that this modular approach will be broadly useful to researchers seeking to capture a specific interaction without having to design an entirely novel probe, using custom chemical synthesis and glycosylation reactions. In our group, we aim to leverage this scaffold along with novel fluorogenic photocrosslinkers to profile glycan recognition in increasingly complex physiological environments such as cells lysates, live cells or biological tissues. Finally, the ability of this trifunctional design to control the valency of the glycan epitope will be studied in future work. Most mammalian lectins show a rather poor affinity for monovalent epitopes and multivalent conjugates bearing glycosylated structures capable of engaging in fluorogenic photocrosslinking may offer a unique advantage for profiling low affinity glycan binding events at the cell surface.

Author contributions

The manuscript was written through contributions of all authors. conceptualization: B. V. Z. and S. C.; synthesis and optimization: B. V. Z. and D. D. C.; photolabeling experiments: B. V. Z. writing and editing: S. C. and B. V. Z.

Conflicts of interest

There are no conflicts to declare.

Data availability

The data supporting this article have been included as part of the supplementary information (SI). Supplementary information: experimental details, synthetic procedures and characterization data. See DOI: <https://doi.org/10.1039/d5cb00206k>.

Acknowledgements

S. C. is a member of the CGCC network (FRQ-Secteur NT – Strategic Clusters, RS-265155), the PROTEO network (FRQ-Secteur NT – Strategic Clusters, 341121) and a GlycoNet network investigator. We gratefully acknowledge the support of the Natural Sciences and Engineering Research Council of Canada (NSERC) for funding this research [RGPIN 2019-05451; DGECR-2019-00076; ALLRP 571434 -21]. We are also grateful to the Fonds de Recherche du Québec – Nature et Technologies (FRQNT) for New Academics support and for equipment support [2021-NC-281486]. We thank the Canada Foundation for Innovation for providing indispensable instrumentation (39336 and 43359). We thank Dr Alexandra Furtos-Matei, Karine Gilbert, Dr Pedro Aguiar, and Dr Cédric Malveau for assistance with mass spectrometry and NMR analyses. Access to the NMR *via* the Regional Centre for Magnetic Resonance (UdeM – Chemistry) was possible thanks to funding from the Canada Foundation for Innovation, the FRQ (RS-265155), and the Institut Courtois.

Notes and references

- 1 A. Varki, R. Cummings, J. Esko, P. Stanley, G. Hart, M. Aebi, D. Mohnen, T. Kinoshita, N. Packer, J. Prestegard, R. Schnaar and P. Seeberger, *Essentials of Glycobiology*, Cold Spring Harbor Laboratory Press, 2022.
- 2 M. Phillips, E. Nudelman, F. Gaeta, M. Perez, A. Singhal, S. Hakomori and J. Paulson, *Science*, 1990, **250**, 1130–1132.
- 3 K. Inamori, T. Yoshida-Moriguchi, Y. Hara, M. E. Anderson, L. Yu and K. P. Campbell, *Science*, 2012, **335**, 93–96.
- 4 M. S. Macauley, P. R. Crocker and J. C. Paulson, *Nat. Rev. Immunol.*, 2014, **14**, 653.
- 5 K. Ohtsubo and J. D. Marth, *Cell*, 2006, **126**, 855–867.
- 6 P. Stanley, *Nat. Rev. Genet.*, 2024, **25**, 715–729.
- 7 C. Reily, T. J. Stewart, M. B. Renfrow and J. Novak, *Nat. Rev. Nephrol.*, 2019, **15**, 346–366.
- 8 S. S. Pinho and C. A. Reis, *Nat. Rev. Cancer*, 2015, **15**, 540.
- 9 J. Poole, C. J. Day, M. von Itzstein, J. C. Paton and M. P. Jennings, *Nat. Rev. Microbiol.*, 2018, **16**, 440–452.
- 10 H. Wu and J. Kohler, *Curr. Opin. Chem. Biol.*, 2019, **53**, 173–182.
- 11 N. D. Pham, R. B. Parker and J. J. Kohler, *Curr. Opin. Chem. Biol.*, 2013, **17**, 90–101.
- 12 H. Wu, A. Shajahan, J.-Y. Yang, E. Capota, A. M. Wands, C. M. Arthur, S. R. Stowell, K. W. Moremen, P. Azadi and J. J. Kohler, *Cell Chem. Biol.*, 2022, **29**, 84–97.
- 13 S.-H. Yu, M. Boyce, A. M. Wands, M. R. Bond, C. R. Bertozzi and J. J. Kohler, *Proc. Natl. Acad. Sci. U. S. A.*, 2012, **109**, 4834–4839.
- 14 N. J. Pedowitz and M. R. Pratt, *RSC Chem. Biol.*, 2021, **2**, 306–321.
- 15 J. L. Babulic and C. J. Capicciotti, *Bioconjugate Chem.*, 2022, **33**, 773–780.
- 16 C. J. Capicciotti, C. Zong, M. O. Sheikh, T. Sun, L. Wells and G.-J. Boons, *J. Am. Chem. Soc.*, 2017, **139**, 13342–13348.



- 17 M. Sojitra, E. N. Schmidt, G. M. Lima, E. J. Carpenter, K. A. McCord, A. Atrazhev, M. S. Macauley and R. Derda, *Nat. Protoc.*, 2025, **20**, 989–1019.
- 18 G. M. Lima, Z. Jame-Chenarboo, M. Sojitra, S. Sarkar, E. J. Carpenter, C. Y. Yang, E. Schmidt, J. Lai, A. Atrazhev, D. Yazdan, C. Peng, E. A. Volker, R. Ho, G. Monteiro, R. Lai, L. K. Mahal, M. S. Macauley and R. Derda, *Chem. Biol.*, 2024, **31**, 1986–2001.
- 19 M. Sojitra, S. Sarkar, J. Maghera, E. Rodrigues, E. J. Carpenter, S. Seth, D. Ferrer Vinals, N. J. Bennett, R. Reddy, A. Khalil, X. Xue, M. R. Bell, R. B. Zheng, P. Zhang, C. Nycholat, J. J. Bailey, C.-C. Ling, T. L. Lowary, J. C. Paulson, M. S. Macauley and R. Derda, *Nat. Chem. Biol.*, 2021, **17**, 806–816.
- 20 J. L. Babulic, F. V. De León González and C. J. Capicciotti, *Curr. Opin. Chem. Biol.*, 2024, **80**, 102456.
- 21 A. A. Hassan, J. M. Wozniak, Z. Vilen, W. Li, A. Jadhav, C. G. Parker and M. L. Huang, *RSC Chem. Biol.*, 2022, **3**, 1369–1374.
- 22 M. E. Griffin and L. C. Hsieh-Wilson, *Cell*, 2022, **185**, 2657–2677.
- 23 K. Sakurai, *Asian J. Org. Chem.*, 2015, **4**, 116–126.
- 24 A. M. Joffrin and L. C. Hsieh-Wilson, *J. Am. Chem. Soc.*, 2020, **142**, 13672–13676.
- 25 K. Sakurai, Y. Hatai and A. Okada, *Chem. Sci.*, 2016, **7**, 702–706.
- 26 N. Suto, S. Kamoshita, S. Hosoya and K. Sakurai, *Angew. Chem., Int. Ed.*, 2021, **60**, 17080–17087.
- 27 H.-J. Gabius, M. Cudic, T. Diercks, H. Kaltner, J. Kopitz, K. H. Mayo, P. V. Murphy, S. Oscarson, R. Roy, A. Schedlbauer, S. Toegel and A. Romero, *ChemBioChem*, 2022, **23**, e202100327.
- 28 A. Varki, *Glycobiology*, 2017, **27**, 3–49.
- 29 C. Bousch, B. Vreulz, K. Kansal, A. El-Husseini and S. Cecioni, *Angew. Chem., Int. Ed.*, 2023, **62**, e202314248.
- 30 M. S. Platz, *Acc. Chem. Res.*, 1995, **28**, 487–492.
- 31 C. Pifferi, G. C. Daskhan, M. Fiore, T. C. Shiao, R. Roy and O. Renaudet, *Chem. Rev.*, 2017, **117**, 9839–9873.
- 32 T. Tanaka, H. Nagai, M. Noguchi, A. Kobayashi and S.-I. Shoda, *Chem. Commun.*, 2009, 3378–3379, DOI: [10.1039/b905761g](https://doi.org/10.1039/b905761g).
- 33 A. Novoa, S. Barluenga, C. Serba and N. Winssinger, *Chem. Commun.*, 2013, **49**, 7608–7610.
- 34 D. Lim, M. A. Brimble, R. Kowalczyk, A. J. A. Watson and A. J. Fairbanks, *Angew. Chem., Int. Ed.*, 2014, **53**, 11907–11911.
- 35 J. Y. Hyun, J. Pai and I. Shin, *Acc. Chem. Res.*, 2017, **50**, 1069–1078.
- 36 M.-r Lee and I. Shin, *Org. Lett.*, 2005, **7**, 4269–4272.
- 37 O. Bohorov, H. Andersson-Sand, J. Hoffmann and O. Blixt, *Glycobiology*, 2006, **16**, 21C–27C.
- 38 F. Peri, P. Dumy and M. Mutter, *Tetrahedron*, 1998, **54**, 12269–12278.
- 39 O. R. Baudendistel, D. E. Wieland, M. S. Schmidt and V. Wittmann, *Chem. – Eur. J.*, 2016, **22**, 17359–17365.
- 40 S. Munneke, J. R. C. Prevost, G. F. Painter, B. L. Stocker and M. S. M. Timmer, *Org. Lett.*, 2015, **17**, 624–627.
- 41 M. Wei, T. R. McKittrick, A. Y. Mehta, C. Gao, N. Jia, A. M. McQuillan, J. Heimbürg-Molinari, L. Sun and R. D. Cummings, *Bioconjugate Chem.*, 2019, **30**, 2897–2908.
- 42 A. R. Prudden, Z. S. Chinoy, M. A. Wolfert and G.-J. Boons, *Chem. Commun.*, 2014, **50**, 7132–7135.
- 43 T. Jia, A. Y. Mehta, C. A. Tilton, E. K. C. Tulin, L. E. Pepi, L. Muerner, S. von Gunten, J. Heimbürg-Molinari, S. R. Stowell and R. D. Cummings, *ACS Cent. Sci.*, 2025, **11**, 753–769.
- 44 A. Iqbal, H. Chibli and C. J. Hamilton, *Carbohydr. Res.*, 2013, **377**, 1–3.
- 45 J. Li, H.-C. Hsu, J. D. Mountz and J. G. Allen, *Cell Chem. Biol.*, 2018, **25**, 499–512.
- 46 M. Schneider, E. Al-Shareffi and R. S. Haltiwanger, *Glycobiology*, 2017, **27**, 601–618.
- 47 G. D. Brown, J. A. Willment and L. Whitehead, *Nat. Rev. Immunol.*, 2018, **18**, 374–389.
- 48 B. Schnider, Y. M'Rad, J. El Ahmadi, A. G. de Brevern, A. Imberty and F. Lisacek, *Nucleic Acids Res.*, 2023, **52**, D1683–D1693.
- 49 Z. Huang, J. I. Park, D. S. Watson, P. Hwang and F. C. Szoka, *Bioconjugate Chem.*, 2006, **17**, 1592–1600.
- 50 A. Audfray, J. Claudinon, S. Abounit, N. Ruvoën-Clouet, G. Larson, D. F. Smith, M. Wimmerová, J. Le Pendu, W. Römer, A. Varrot and A. Imberty, *J. Biol. Chem.*, 2012, **287**, 4335–4347.

